

53

Presentation date: Juny, 2024
Date of acceptance: October, 2024
Publication date: December, 2024

ENVIRONMENTAL

SUSTAINABILITY: A PROPOSAL BASED ON CO₂ REMOVAL AND ADVANCED MATERIAL SYNTHESIS

SOSTENIBILIDAD AMBIENTAL: UNA PROPUESTA BASADA EN LA ELIMINACIÓN DE CO₂ Y LA SÍNTESIS DE MATERIALES AVANZADO

María Isabel González-Nava ^{1*}

E-mail: mgonzalez304@alumnos.uaq.mx

ORCID: <https://orcid.org/0009-0000-3161-6105>

Rufino Nava-Mendoza ¹

E-mail: rufino@uaq.mx

ORCID: <https://orcid.org/0000-0001-7230-073X>

Angelica Rosario Jiménez Sánchez ¹

E-mail: rosariojs@uaq.mx

ORCID: <https://orcid.org/0000-0002-4950-4221>

Jorge Domingo Mendiola Santibañez¹

E-mail: mendijor@uaq.mx

ORCID: <https://orcid.org/0000-0002-9173-0732>

Israel Santillán ²

E-mail: israel.sm@lapaz.tecnm.mx

ORCID: <https://orcid.org/0000-0003-0027-7176>

¹Universidad Autónoma de Querétaro, Querétaro. México.

² National Technological Institute of México, La Paz Campus, México.

* Author for correspondence

Suggested citation (APA, seventh ed.)

González-Nava, M. I., Nava-Mendoza, R., Jiménez Sánchez, A. R., Mendiola Santibañez, J. D. & Santillán, I. (2024). Environmental sustainability: a proposal based on CO₂ removal and advanced material synthesis. *Universidad y Sociedad*, 16(S2), 501-513.

ABSTRACT

The concern of scientists and climatologists that high greenhouse gas emissions are on the rise, causing the earth's surface to warm at a very rapid rate (Maring & Webley, 2013), have required solutions and technologies to reduce these emissions. By capturing, storing and transforming carbon dioxide (CO₂), there is an opportunity to reduce emissions into the atmosphere and mitigate related problems. The following research describes the processes that were carried out to adsorb CO₂, starting with the synthesis of mesoporous silica (SBA-15). MgO, Mg (OH)₂, CaO y Ca (OH)₂ in proportions of 5%, 10% and 15%, were impregnated in SBA-15, continuing with the studies to know that the impregnation was correct and to continue the adsorption process. According to the results and analyzing the samples of MgO, Mg (OH)₂, CaO y Ca (OH)₂, which are supported in the SBA-15, those with the highest CO₂ adsorption are magnesium, which increases the higher the proportion of impregnation for 15% MgO, 4.5 mmol/g and 4.1 mmol/g for 15% Mg(OH)₂.

Keywords: CO₂ adsorption, Acetates, Oxides, Hydroxides, Mesoporous silica.

RESUMEN

La preocupación de científicos y climatólogos debido a que las altas emisiones de gases de efecto invernadero van en aumento provocando que la superficie de la tierra se caliente a un ritmo muy acelerado (Maring & Webley, 2013), han requerido de soluciones y tecnologías para reducir estas emisiones. Mediante la captura, almacenamiento y transformación de dióxido de carbono (CO₂) se tiene la oportunidad de reducir las emisiones a la atmósfera y mitigar los problemas relacionados. La siguiente investigación describe los procesos que se llevaron a cabo para adsorber CO₂, comenzando con la síntesis de la sílice mesoporosa (SBA-15). Los MgO, Mg (OH)₂, CaO y Ca (OH)₂ en proporciones de 5 %, 10 % y 15 %, se impregnaron en la SBA-15, continuando con los estudios para saber que la impregnación fue

correcta y continuar el proceso de adsorción. De acuerdo con los resultados y analizando las muestras del MgO, Mg (OH)₂, Ca O y Ca (OH)₂, mismas que se encuentran soportadas en la SBA-15, las de mayor adsorción de CO₂ son las de magnesio, el cual va en aumento mientras mayor sea la proporción de la impregnación para un 15 % de MgO, 4.71 mmol/g y 4.1 mmol/g para 15 % de Mg (OH)₂.

Palabras clave: Adsorción de CO₂, Acetatos, Óxidos, Hidróxidos, Sílice mesoporosa.

INTRODUCTION

Human activity has caused CO₂ emissions to be emitted in large quantities into the atmosphere and seriously affect the environment and people's quality of life. It is estimated that without CO₂ and water vapor in the atmosphere, the average temperature at the Earth's surface would be below zero, as these gases absorb some of the infrared radiation that goes back into space after bouncing off the Earth's surface (Zeyad et al., 2022). In this way, if carbon emissions are not drastically reduced, there will be irreparable damage to the planet, but what if there was a way to repair all this damage?

To capture CO₂, it is necessary to separate it from the rest of the gases that originate during combustion in processes that are carried out in industries, thermoelectric plants, and many more. When separated from the other gases, it is transferred and introduced into deep geological formations where it will be isolated, it is in this way that the amount of CO₂ generated in the atmosphere can be minimized (López et al., 2013).

According to Cuellar et al. (2015), the process of transforming CO₂ is based on the chemical conversion that occurs with alkaline adsorbents. Since there is a sustainable approach to the permanent storage of CO₂, the transformation of CO₂ into calcium and magnesium carbonates must be stable and insoluble in water (Shan et al., 2018). Adsorption, on the other hand, is the method of transferring a material known as an adsorbate from a liquid or gas to a solid phase called an adsorbent (Adamson, 1996). In this process, the adsorbent material is a porous solid that helps keep the adsorbate on its surface (Beruto & Botter, 2000).

Some alkaline adsorbents have been proposed for CO₂ capture such as simple metal oxides (e.g., CaO, MgO), hydroxides (e.g., Ca (OH)₂, Mg (OH)₂, and Na (OH)₂ (Reddy et al., 2011). They consist of particles of base metals which are needed in nanoscale sizes (Gislason et al., 2014). Calcium hydroxide can be used as a reagent (Vance et al., 2015), calcium and magnesium

oxides facilitate carbonate formation by reacting with CO₂ (Cuellar et al., 2015) and are silicate minerals, which are relatively abundant worldwide, making them an attractive feedstock for CO₂ mineralization (Styring & North, 2015). In this case, the material called SBA-15 (Santa Barbara Amorphous No. 15), which was first developed by Stucky et al. (1994), to which, due to its textural properties, nanoparticles of hydroxides and oxides can be incorporated (as in this case), which causes them to have a high dispersion and consequently much more active adsorbents are generated. It has a high surface area and a hexagonal structure of uniform pores (honeycomb-like), and in addition, a wide range of pore sizes (4.6 nm to 30 nm) and pore wall thicknesses (3.1 nm to 6.4 nm).

In this work, we seek to develop CO₂ adsorbent materials based on mesoporous silicas of the SBA-15 type decorated with nanoparticles of hydroxides and oxides of calcium and magnesium, for the capture and conversion of CO₂, due to the efficiency of CO₂ adsorption that is had with the resulting material, it can be implemented in the use of cementitious processing for its capture, as well as the generation of fuel from the capture of CO₂, at the same time as helping not to pollute with gas, it can be used in the creation of new materials that are used in the daily life of society.

MATERIALS AND METHODS

Material Preparation

Synthesis of the ordered mesoporous silica material SBA-15

The short SBA-15 mesoporous silica material was prepared using the Sol-Gel process (Zarazua et al., 2017), where a neutral surfactant is used as the directing agent of the mesostructure, Pluronic P123.

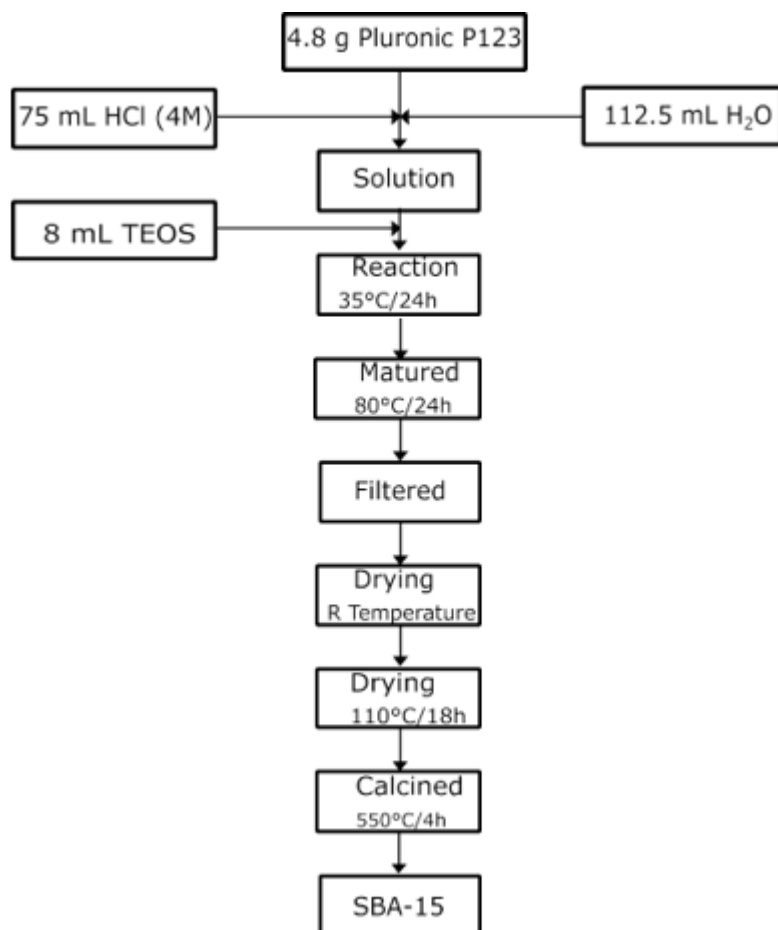
P123 is dissolved in a solution of hydrochloric acid and deionized water with constant agitation at 35°C. Once P123 is completely dissolved, the Sol-Gel process begins by adding the silica precursor (Hernández et al., 2014) TEOS. The reaction was performed for 24 hours and with constant agitation.

After this time, the maturation process is carried out, placing the gel obtained in a polypropylene container, covering it and placing it in the muffle for 24 hours at a temperature of 80°C without stirring.

When finished, it is allowed to cool and the solid is recovered by filtration (Styring & North, 2015). It is dried at room temperature and then at 110°C for 18 hours at a heating rate of 2°C/min.

Finally, it is calcined at 550°C for 4 hours at a heating rate of 1°C/min. In this way, it will be possible to eliminate the organic base by producing only the mesoporous silica structure (Vance et al., 2015). The process is described in the figure below (Figure 1).

Fig 1. Synthesis of Ordered Mesoporous Silica Material SBA-15.



Source: own elaboration.

Incorporation of Ca (OH)₂ and Mg (OH) nanoparticles into SBA-15.

For the incorporation of calcium hydroxide (Ca (OH)₂) and magnesium hydroxide (Mg (OH)₂) nanoparticles into the surface of SBA-15 mesoporous silica, the pore-filling impregnation method (incipient wetting) was used (Feliczak et al., 2016). Calcium and magnesium hydroxides, aqueous solutions of calcium (II) acetate dihydrate Ca (OH)₂•2H₂O (Sigma-Aldrich) and magnesium (II) acetate dihydrate Mg (OH)₂•2H₂O (Sigma-Aldrich) were used as sources. The amounts (5, 10 and 15 % by weight) of Ca (OH)₂ and Mg (OH)₂ and (5, 10 and 15 % by weight) of CaO and MgO that were deposited in the SBA-15 were varied. Subsequently, the impregnated samples were dried at a temperature of 110°C for 18h.

Material characterization

Determination of the textural, morphological, structural and electronic properties of adsorbent materials:

Adsorption-desorption isotherms from N₂ to 77 K

The textural properties of the mesoporous silicas SBA-15 and NH₂-SBA-15 were determined by adsorption-desorption isotherms from N₂ to 77 K in an Autosorb iQ2 equipment, of the Quantachrome brand.

Prior to analysis, the sample was degassed at 150°C in vacuum for 5 h, to ensure a dry, clean surface free of weakly adsorbed species.

X-ray diffraction (XRD) at low and conventional angles

By X-ray diffraction (XRD) at low angles ($0-5^\circ$ at 2θ), the order in the pore arrangement of SBA-15C and NH_2 -SBA-15C was verified (Tanev & Pinnavaia, 1995).

Scanning Electron Microscopy (SEM)

The HITACHI SU8200 scanning electron microscope was used to image the SBA-15 and NH_2 -SBA-15 samples, mainly to determine the morphology and size of the particles (Chang, 2017 b).

The pellet-shaped samples will be placed in the sample holders and coated with charcoal.

Fourier transform infrared spectroscopy (FT-IR)

The presence of the amino groups on the surface of the mesoporous silica SBA-15, as well as the interaction of the CO_2 molecule with the amino groups, were analyzed by means of the vibrational response of their molecular bonds, through infrared spectroscopy analyses (Beck et al., 2008). The IR vibration spectra of the powder samples will be measured on a Bruker Vector 33 spectrophotometer, in the range of 400 to 4000 cm^{-1} , with a resolution of 2 cm^{-1} .

Micro Raman spectroscopy

The vibronic spectra of the molecular bonds due to the presence of the amino groups in the NH_2 -SBA-15 samples and as a complementary characterization to the FT-IR spectra, micro-Raman spectroscopy was performed, using a Labram-Dior model micro spectrometer (López, 2013).

Thermogravimetric Analysis (TGA)

The TGA/DTG thermogravimetric analysis will allow the evaluation of the thermal stability of the amino functional groups inside the pores of mesoporous materials (Montes et al., 2012). This study will be carried out on a TA Instruments Q500 TGA and Q2000 DSC equipment, in a temperature range of 25 °C to 600 °C.

Carbonation reaction

The carbonation reaction under non-isothermal conditions was carried out in a TGA/DTG thermogravimetric analyzer, in a Q500 TGA equipment from TA Instruments, in a temperature range of 25°C to 800°C. With a heating speed of 10°C/min and a flow of 50 mL/min of 100% CO_2 gas.

Determination of the type of interaction between hydroxide nanoparticles and calcium and magnesium oxide.

X-ray photoelectron spectroscopy (XPS)

The XPS technique allows the species in a sample to be identified, their oxidation state and their chemical environment. Because each atom has a characteristic response factor, the XPS signal can be used in the quantitative determination of chemical species on the surface (Zhao et al., 1998).

To verify the adsorption of CO_2 molecules in the adsorbents, X-ray photoelectron spectroscopy (XPS) was performed.

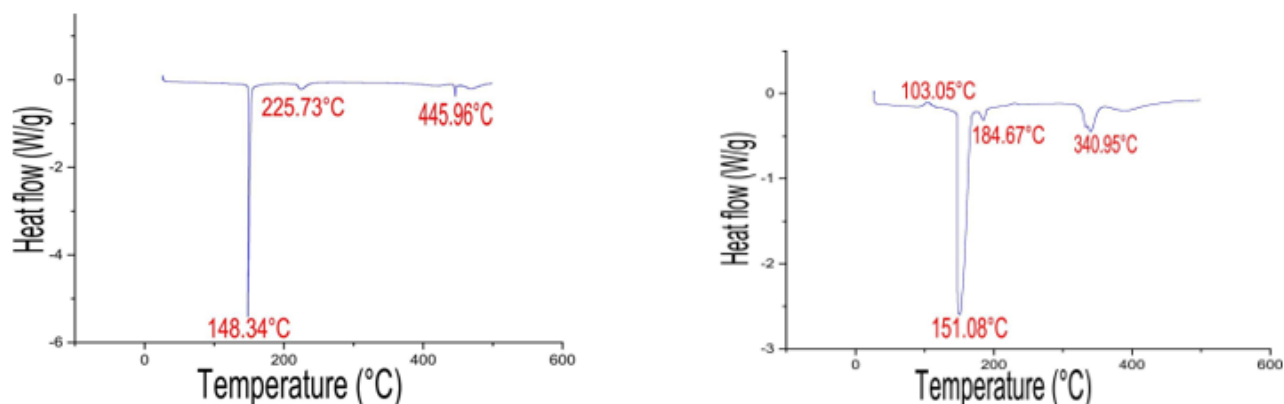
RESULTS-DISCUSSION

Differential Scanning Calorimetry (DSC)

Hydroxides are obtained from 100°-300°, in our case calcium hydroxides were obtained at 148.34° and magnesium hydroxides at 151.08, while oxides are obtained from 301°-500°, calcium oxides were at 445.96° and magnesium oxides at 340.95° (Figure 2).

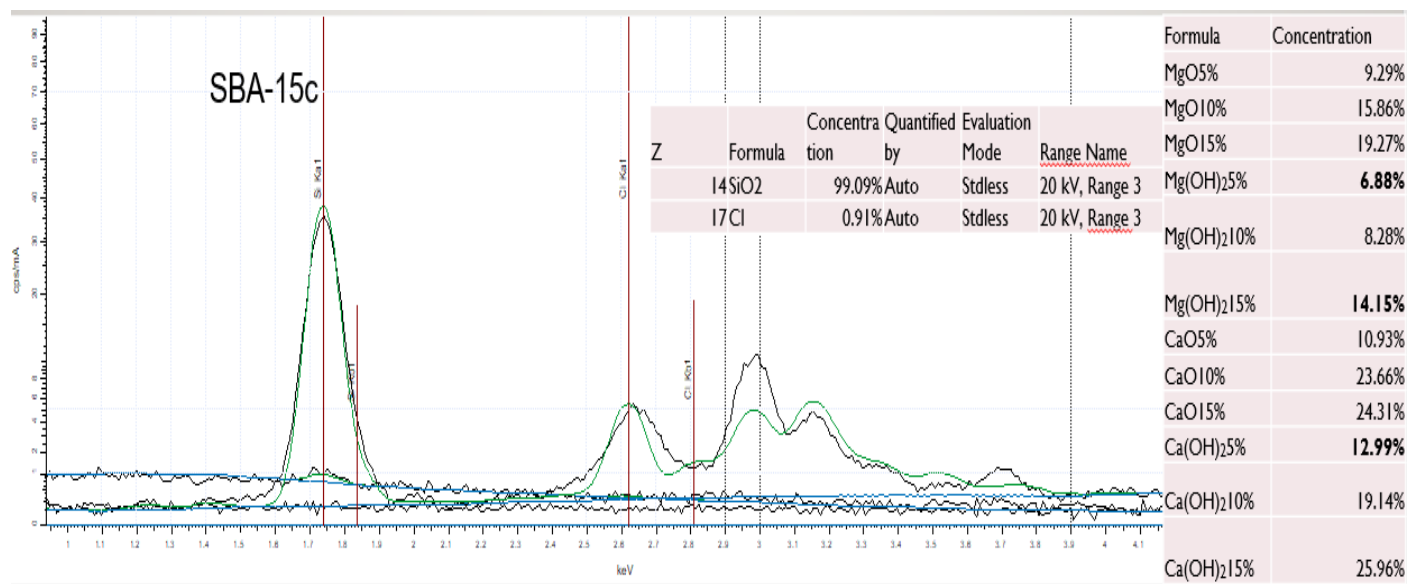
The precursors of Ca and Mg impregnated in SBA-15, which were given a heat treatment of 110°C. It was determined with greater precision to know at what temperature the hydroxides and oxides of calcium and magnesium are obtained, according to what has been reported in the literature.

Fig. 2. Profiles of DSC of the hydroxides and oxides of calcium and magnesium.



Source: own elaboration.

You can see that the proportions of the samples are above the percentages indicated, so the results will be excellent when adsorbing the CO₂ with our materials (Figure 3).

 Fig 3. Note that the samples' proportions are above the indicated percentages, so the results will be excellent when adsorbing the CO₂ with our materials.


Source: own elaboration.

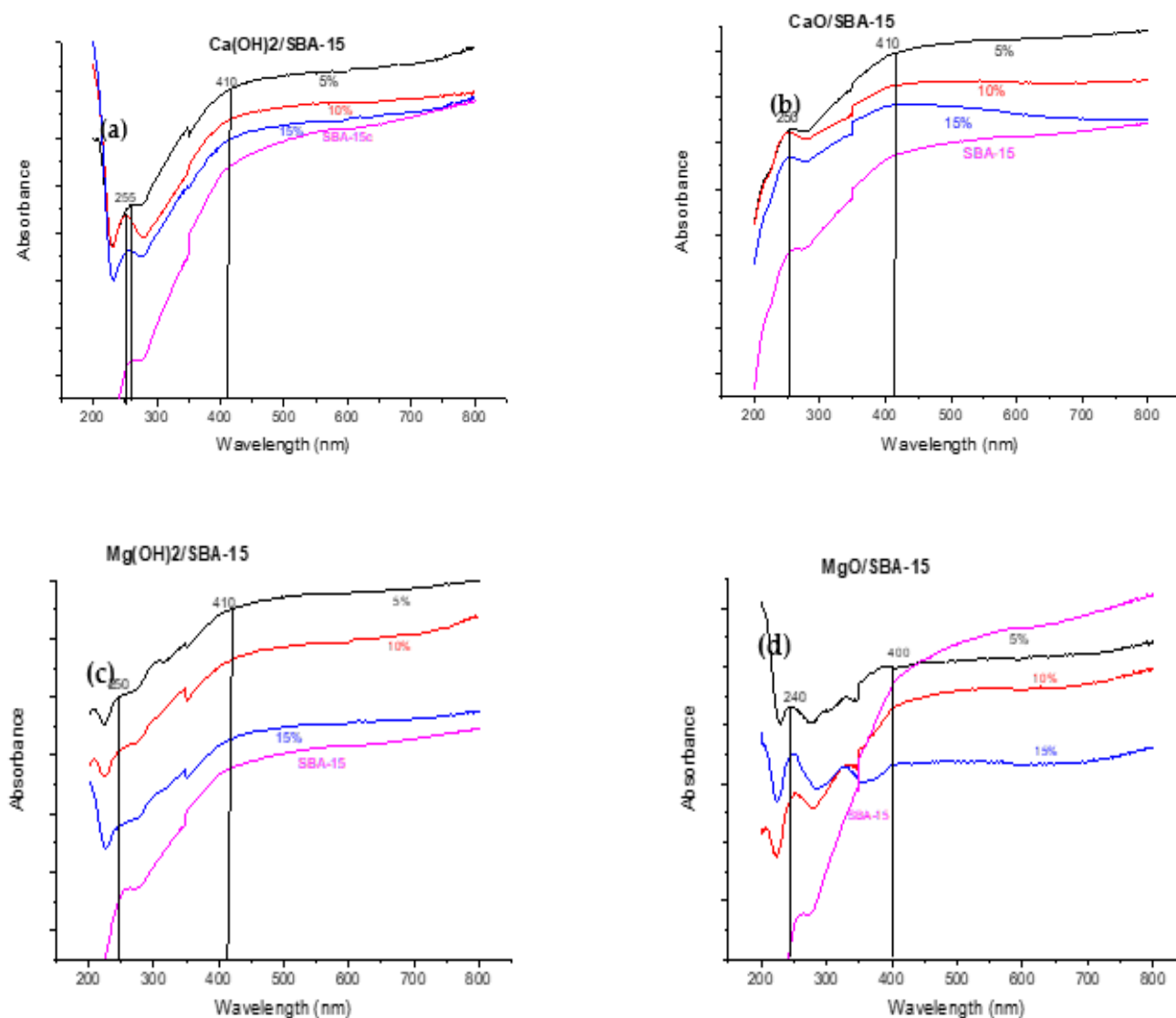
Pure mesoporous silica (SBA-15) and the different results with respect to the equivalent proportion of each of the precursors, starting with magnesium oxides, of 5%, 10% and 15%, magnesium hydroxides, of 5%, 10% and 15%, calcium oxides, of 5%, 10% and 15%, and calcium hydroxides, of 5%, 10% and 15%, which are in an adequate proportion.

Diffuse reflectance spectroscopy in the Uv-vis range

Figure 4: a) Two high-intensity absorption bands centered at approx. 255 and 360 nm, characteristic of OH-bound Ca²⁺, at the edges and corners of Ca(OH)₂ crystallites. b) Two absorption bands with high intensity, approx. at 250 and 350 nm, characteristic of Ca²⁺ bound to O²⁻, at the edges and corners of the CaO crystallites. c) Two absorption bands with high intensity, approx. at 250 and 330 nm, characteristic of Mg²⁺ bound to OH⁻, at the edges and corners of the Mg(OH)₂ crystallites, d) Two absorption bands with high intensity, approx. at 250 and 330 nm, characteristic of Mg²⁺

bound to O²⁻, at the edges and corners of the MgO crystallites. These bands indicate the presence of hydroxides and oxides of calcium and magnesium.

Fig 4. Diffuse reflectance spectroscopy in the uv-vis range.



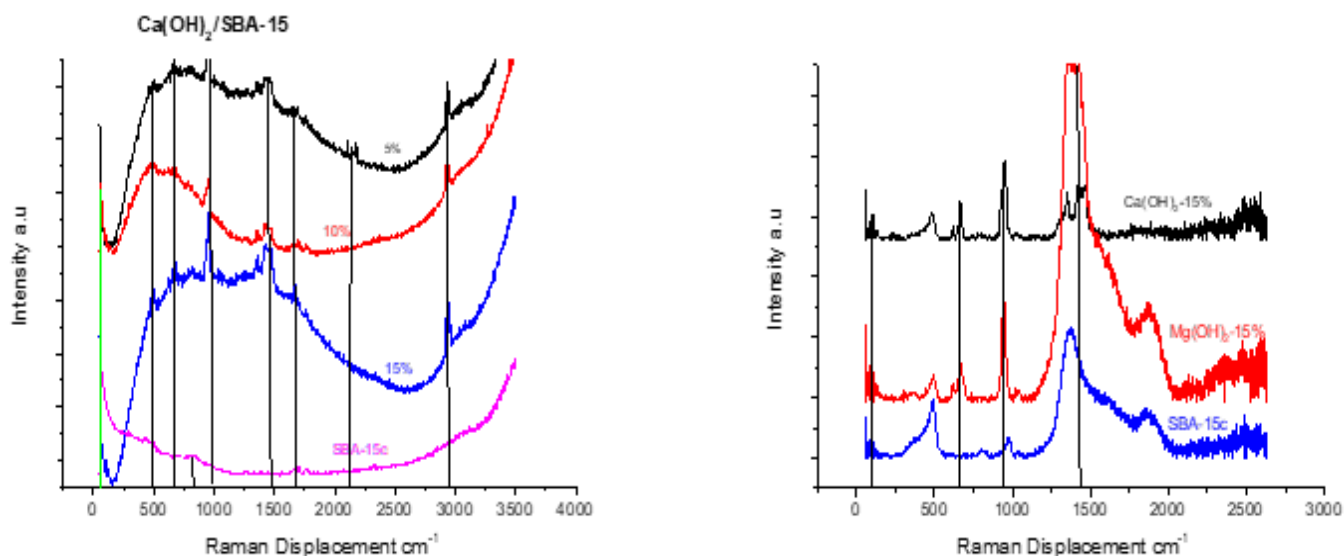
Source: own elaboration.

Espectroscopia micro-Raman

Figure 5: In the figure on the left, peaks are observed in the spectra at the positions of 80 cm⁻¹, 500 cm⁻¹, 700 cm⁻¹, 1000 cm⁻¹, 1500 cm⁻¹, 1700 cm⁻¹ and 3000 cm⁻¹ approximately assigned to the vibration modes respectively. These optical modes are characteristic of the hexagonal structure. In the figure on the right, peaks are observed in these spectra at the positions of 80 cm⁻¹, 500 cm⁻¹, 700 cm⁻¹, 1000 cm⁻¹, 1500 cm⁻¹, 1700 cm⁻¹ and 1900 cm⁻¹ approximately assigned to the vibration modes respectively.

As in the diffuse UV-VIS reflectance, the micro-Raman study confirms the presence of hydroxides and oxides of calcium and magnesium. Charges (wavenumbers) are displayed.

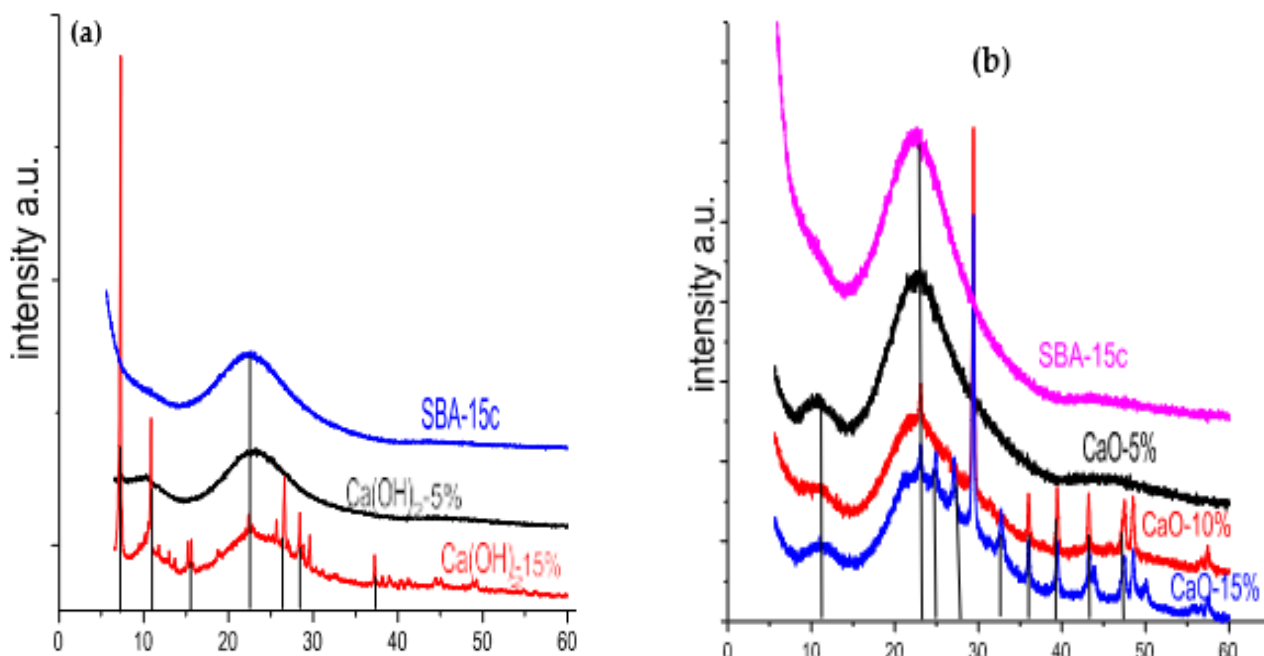
Fig. 5. Espectroscopia micro-Raman.



Source: own elaboration.

X-ray Diffraction (XRD)

It can be seen in the images of paragraphs a and b, that the reflections that are presented are longer, but shorter, while in the image of section c a pronounced reflection is seen different from that of pure esoporous silica, which indicates the existence of Mg (OH)₂, impregnated, the same happens in section d with MgO, therefore, in all the samples analyzed, hydroxides and oxides of calcium and magnesium were successfully impregnated (Figure 6).

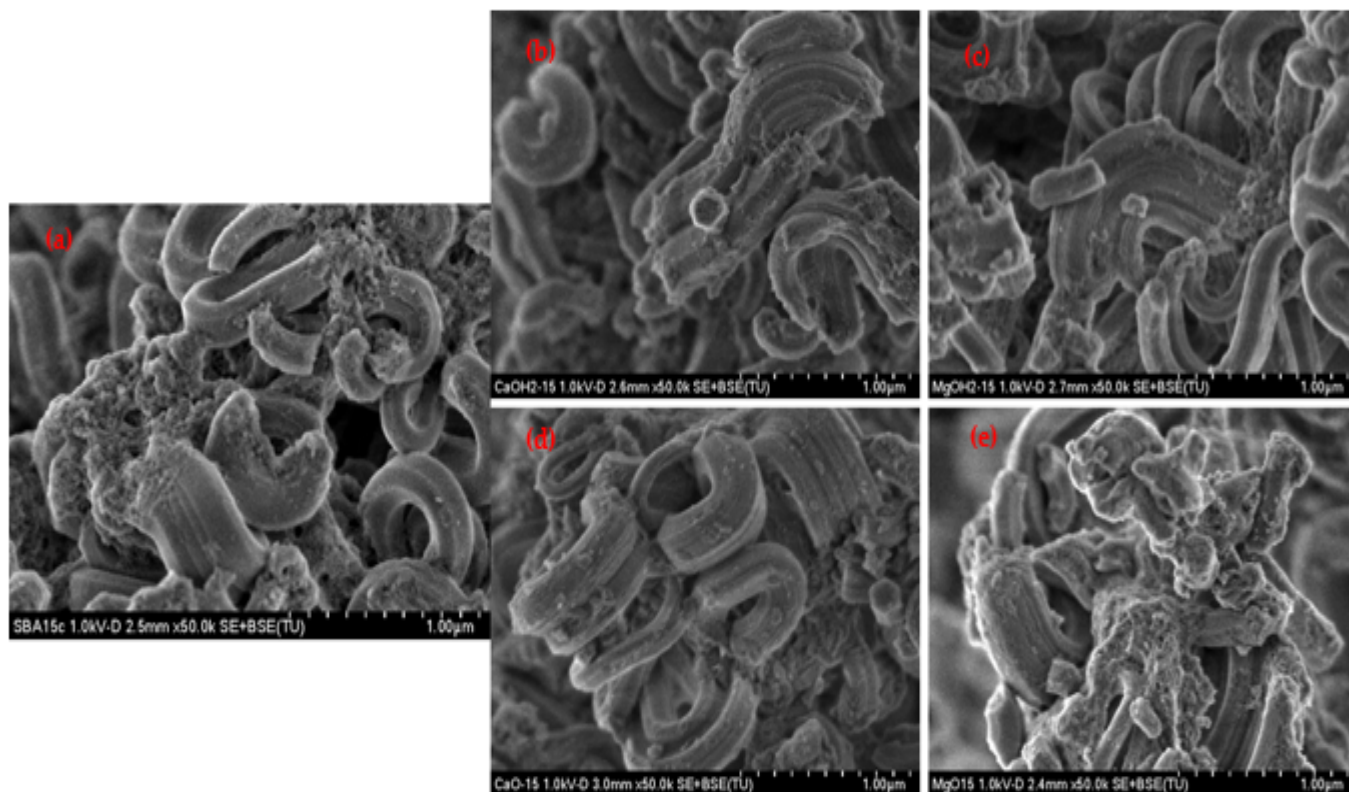
Fig. 6. X-ray diffraction (XRD): a) Ca (OH)₂, b) Ca O, c) Mg (OH)₂ and d) MgO.

Source: own elaboration.

SEM

Figure 7. a) SBA-15, b) Ca (OH)₂, c) Mg (OH)₂, d) CaO and e) MgO.

Fig 7. Sem.



Source: own elaboration.

Even with the impregnation of calcium and magnesium hydroxides and oxides, the structure of SBA-15 is preserved. In all the images particles are observed with the naked eye that are not seen in SBA-15, which comparing it with the other methods that were carried out tells us that there is the presence of calcium and magnesium, these are found on the external surface, in figure d, it can be seen that there is a greater surface area so it is very likely that the CaO, are impregnated on the inner surface of the pores.

Infrared Spectroscopy

Figure 8. The following bands indicate us:

750-800 cm⁻¹, is assigned to the vibration of the Si-O-Si bond, siloxane group.

950 cm⁻¹ Si-OH siranol group.

1100 cm⁻¹ Si-O-Si siloxane group.

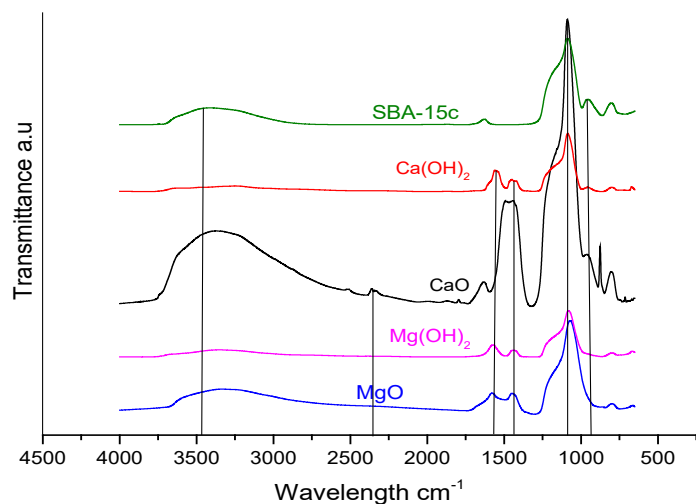
1600 cm⁻¹ water adsorbed on the material.

2300 cm⁻¹ interaction between CaO and Si.

3500 cm⁻¹ Si-OH siranol group.

It is confirmed with the Micro Raman analysis that the higher the percentage, the larger the wavenumbers.

Fig. 8 Infrared Spectroscopy.



Source: own elaboration.

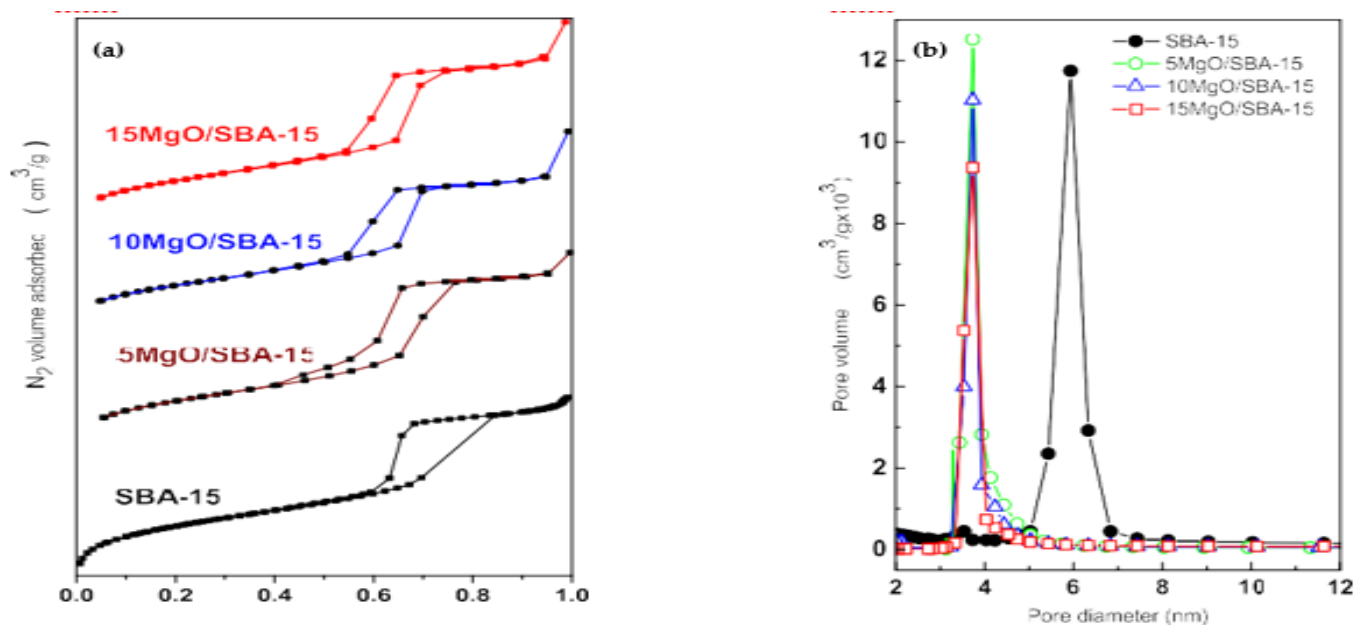
MgO and CaO isotherms/ Pore size distribution of MgO and CaO.

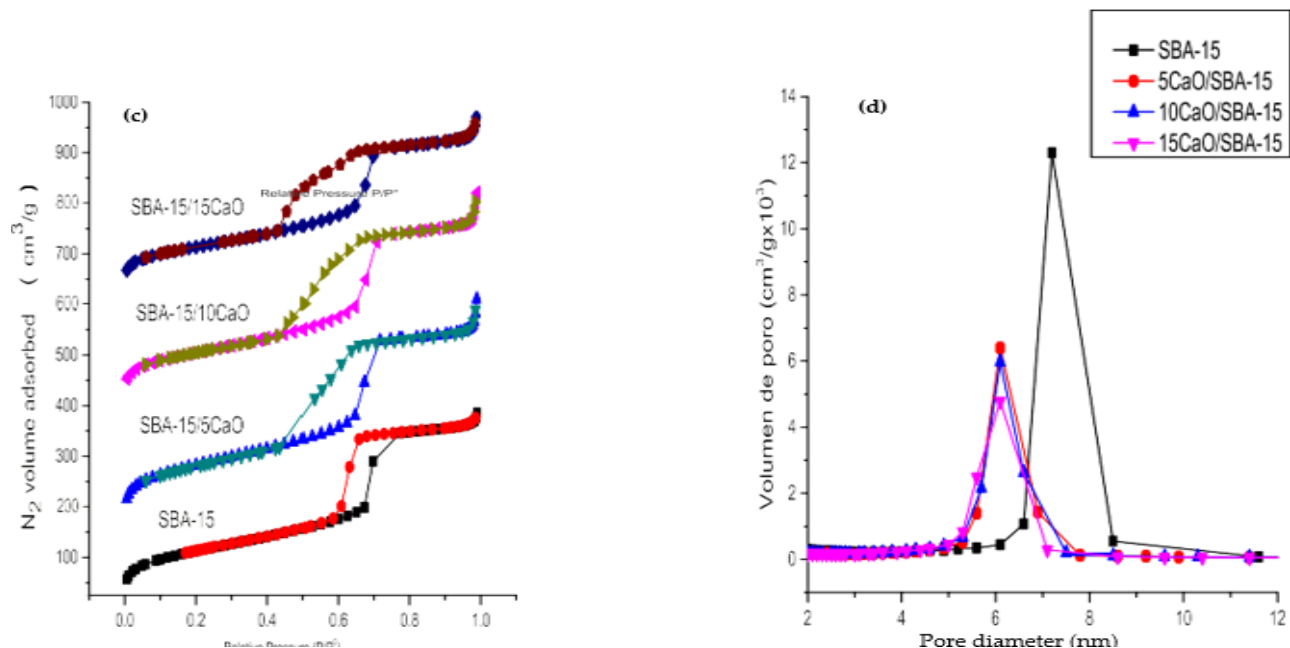
Figure 9. Left-sided MgO and CaO isotherms/ Right-sided MgO and CaO pore size distribution.

The textural properties of mesoporous materials were studied by means of the N_2 adsorption-desorption isotherms at 77 K. Pore size distributions were calculated from the adsorption isotherm using the Barrett-Joyner-Halenda model.

The N_2 adsorption-desorption isotherms of the materials are shown in Fig. 9, on the left side. All mesoporous samples of MgO/SBA-15 and CaO/SBA-15, as well as pure SBA-15, exhibit type IV adsorption isotherms with areas of type H1 hysteresis according to the IUPAC classification. These isotherms are characteristic of mesoporous materials with a hexagonal arrangement of pores.

Fig. 9. Left-sided MgO and CaO isotherms/ Right-sided MgO and CaO pore size distribution.





Source: own elaboration.

The SBA-15 sample presents the hysteresis area in a well-defined range at high relative pressures ($0.61 < P/P_0 < 0.8$) representing spontaneous filling of mesopores due to capillary condensation, indicating the presence of uniform mesopores. Modified mesoporous silicas of MgO and CaO show areas of hysteresis at intervals of lower relative pressures ($0.4 < P/P_0 < 0.7$) due to a decrease in the size of the mesopores due to the presence of small particles of MgO and CaO dispersed within the pores of SBA-15.

All the isotherms presented are similar to those reported in the literature for the mesoporous silica SBA-15. As seen in Fig. 9, on the left side, the N_2 adsorption-desorption isotherms of the mesoporous matrices (MgO)/SBA-15 and (CaO) x/SBA-15 are similar, indicating that the mesostructure of the SBA-15 material was maintained after the incorporation of MgO and CaO.

Regarding the pore size distribution shown in Fig. 9, on the right side it should be noted that all mesoporous matrices show a uniform and narrow pore size distribution. There appears to be a change in pore diameter to a smaller diameter following an increase in MgO and CaO loading. Simultaneously, the total volume of N_2 decreased with the increase in the load of MgO and CaO in the mesoporous matrices. As expected, the loading of magnesium and calcium in the silica matrix decreases the surface area and pore volume of the SBA-15 support (Table 1).

As the Mg and CaO load increases, there is a change from diameter to smaller and the total volume also decreases.

Table 1. Textural properties of SBA-15, MgO/SBA-15 and CaO/SBA-15 mesoporous materials.

| Sample | MgO y CaO(wt.%) | SBET(m ² /g) | Vtotal(m ³ /g) | Dp (nm) | Adsorption (mmol/g) | | | | | | |
|---------------|-----------------|-------------------------|---------------------------|---------|---------------------|--|--|--|--|--|--|
| SBA-15 | 0.0 | 932 | 1.05 | 5.9 | 0 | | | | | | |
| 5%MgO/SBA-15 | 9.29 | 659 | 0.83 | 5.0 | 3.42 | | | | | | |
| 10%MgO/SBA-15 | 15.86 | 505 | 0.69 | 5.0 | 3.96 | | | | | | |
| 15%MgO/SBA-15 | 19.27 | 507 | 0.52 | 4.1 | 4.71 | | | | | | |
| 5%CaO/SBA-15 | 10.93 | 584 | 0.694 | 5.1 | 3.1 | | | | | | |
| 10%CaO/SBA-15 | 23.66 | 575 | 0.683 | 4.9 | 3.4 | | | | | | |
| 15%CaO/SBA-15 | 24.31 | 506 | 0.581 | 4.0 | 3.85 | | | | | | |

Source: own elaboration.

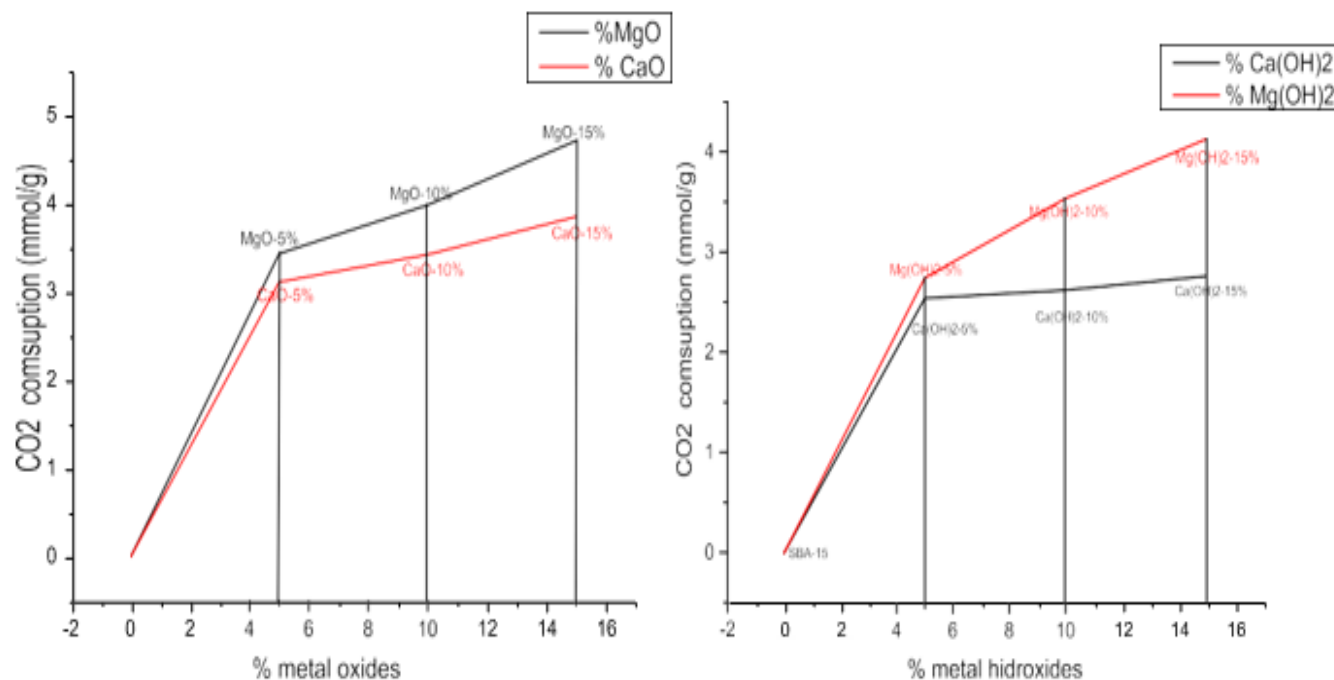
BET Specific Surface Area (SBET), Total Pore Volume (Vtotal) and Pore Diameter (Dp)

CO₂ Adsorption. TGA

Figure 10: Adsorption of CO₂, on the left side calcium and magnesium oxides in proportions of 5%, 10% and 15%, on the right-side calcium and magnesium hydroxides in proportions of 5%, 10% and 15.

According to the study carried out, we can see that the higher the percentage of impregnation of calcium and magnesium oxides and hydroxides, their absorbance increases, but the material that presents the highest CO₂ adsorption is magnesium.

Fig: 10. Adsorption of CO₂.



Source: own elaboration.

CONCLUSIONS

The mesoporous silica material SBA-15 was successfully prepared by the Sol-Gel process with a neutral surfactant as the directing agent of the mesostructure, Pluronic P123.

The results of XRD, Micro Raman and FTIR indicated the presence of calcium and magnesium oxides and hydroxide nanoparticles in SBA-15.

SBET (pore diameter distribution) results indicated that magnesium oxide nanoparticles are dispersed on the inner surface of the pores of SBA-15.

The XRD results indicated a high dispersion of hydroxides and magnesium oxides in SBA-15, generating a higher density of active sites for CO₂ adsorption and therefore a higher CO₂ consumption.

The higher the percentage of impregnation of calcium and magnesium oxides, the higher the CO₂ consumption.

According to the studies carried out, it can be seen that the material that is supported in the mesoporous silica of the SBA-15 type with greater CO₂ adsorption is magnesium, and which increases the higher the proportion of the impregnation, for 15% of MgO, 4.71 mmol/g and 4.1 mmol/g for 15% of Mg(OH)₂.

REFERENCES

- Adamson A. (1996). Physical adsorption of vapors: Three personae. *Colloids and Surfaces a: Physicochemical and Engineering Aspects*, 118(3), 193-201. [https://doi.org/10.1016/S0927-7757\(96\)03684-9](https://doi.org/10.1016/S0927-7757(96)03684-9)
- Beck, A., Horváth, A., Stefler, G., Katona, R., Geszti, O., Tolnai, G., ... & Guczi, L. (2008). Formation and structure of Au/TiO₂ and Au/CeO₂ nanostructures in mesoporous SBA-15. *Catalysis Today*, 139(3), 180-187. <https://www.sciencedirect.com/science/article/abs/pii/S0920586108002691>
- Beruto, D. T. & Botter, R. (2000). Liquid-like H₂O adsorption layers to catalyze the Ca(OH)₂/CO₂ solid-gas reaction and to form a nonprotective solid product layer at 20°C. *Journal of the European Ceramic Society*, 20(4), 497-503. [http://dx.doi.org/10.1016/S0955-2219\(99\)00185-5](http://dx.doi.org/10.1016/S0955-2219(99)00185-5)
- Cuellar Bermúdez, S. P., García, S., Rittmann, B., & Parra, R. (2015). Photosynthetic bioenergy from CO₂: an approach to flue gas harvesting for third-generation biofuels. *Journal of Cleaner Production*, 98, 53-65. <https://doi.org/10.1016/j.jclepro.2014.03.034>
- Chang, R., S. Kim, S. Lee, S. Choi, M. Kim, and Y. Park. 2017b. Calcium carbonate precipitation for CO₂ storage and utilization: A review of the carbonate crystallization and polymorphism. *Frontiers in Energy Research* 5(17). doi: 10.3389/fenrg.2017.00017.
- Feliczak-Guzik, A., Jadach, B., Piotrowska, H., Murias, M., Lulek, J., Nowak, I. (2016). Synthesis and characterization of SBA-16 mesoporous materials containing amine groups. *Microporous and Mesoporous Materials*, 220(15), 231-238. <https://doi.org/10.1016/j.micromeso.2015.09.006>
- Gislason, S., Broecker, W. S., Gunnlaugsson, E., Snæbjörnsdóttir, S., Mesfin, K. G., Alfredsson, H. A., Aradóttir, E. S., Sigfusson, B., Gunnarsson, I., Stute, M., Matter, J. M., Arnarson, M. Th., Galeczka, I. M., Gudbrandsson, S., Stockman, G., Wolff-Boenisch, D., Stefansson, A., Ragnheidardóttir, E., Flaathen, T., Gysi, A.P., Olssen, J., Didriksen, K., Stipp, S., Menez, B., & Oelkers, E. H. (2014). Rapid solubility and mineral storage of CO₂ in basalt. *Energy Procedia*, 63, 4561-4574. <https://doi.org/10.1016/j.egypro.2014.11.489>
- Hernández Barrios, C. A., Duarte Peñaranda, N. Z., Hernández Eugenio, L. M., Peña Ballesteros, D. Y., Coy Echeverría, A. E., & Viejo Abrante, F. (2013). Síntesis, caracterización y evaluación de recubrimientos híbridos porosos sol-gel dopados con acetato de cerio sobre la aleación de magnesio WE54-AE. *Iteckne*, 10(2), 249-258. http://www.scielo.org.co/scielo.php?pid=S1692-17982013000200013&script=sci_arttext
- López, J. C., Quijano, G., Souza, T. S., Estrada J., Lebrero, R., & Muñoz, R. (2013). Biotechnologies for the reduction of greenhouse gases (CH₄, N₂O and CO₂): state of the art and challenges. *Appl Microbiol Biotechnol*, 97(6), 2277-303. <https://doi.org/10.1007/s00253-013-4734-z>
- Maring, B., & Webley, P. (2013). A new simplified pressure/vacuum oscillation adsorption model for rapid adsorbent detection for CO₂ Capture Applications. *International Journal of Greenhouse Gas Control*, 15, 16-31. <https://doi.org/10.1016/j.ijggc.2013.01.009>
- Montes Hernández, G., R. Chiriach, F. Toche, & F. Renard. (2012). Gas-solid carbonation of Ca(OH)₂ and CaO particles under non-isothermal and isothermal conditions by using a thermogravimetric analyzer: Implications for CO₂ capture. *International Journal of Greenhouse Gas Control*, 11, 172-180. <https://www.sciencedirect.com/science/article/abs/pii/S1750583612001946>
- Reddy, K. J., John, S., Weber, H., Argyle, M. D., Bhattachryya, P., Taylor, D. T., Christensen, M., Foulke, T., & Fahlsing, P. (2011). Simultaneous capture and mineralization of coal combustion flue gas carbon dioxide (CO₂). *Energy Procedia*, 4, 1574-1583. <https://doi.org/10.1016/j.egypro.2011.02.027>
- Shan, Y., Guan, D., Zheng, H., Ou, J., Li, Y., Meng, J., Mi, Z., Liu, Z & Zhang, Q. (2018). China's CO₂ Emissions Accounts 1997-2015. *Sci Data*, 5(170201). <https://doi.org/10.1038/sdata.2017.201>
- Stucky, G. D., Huo, Q., Firouzi, A., Chmelka, B., Schacht, S., Voigt, I. G., Schüth, F. (1994). Directed Synthesis of organic/inorganic composite structures. *Studies in Surface Science and Catalysis*, 105, 3-28. [https://doi.org/10.1016/S0167-2991\(97\)80534-4](https://doi.org/10.1016/S0167-2991(97)80534-4)
- Styring P., & North, M. (2015). Perspectives and visions on CO₂ capture and utilization. *Faraday Discussions*, 183, 489-502. <https://doi.org/10.1039/C5FD90077H>
- Tanev, P. T., & Pinnavaia, T. J. (1995). A neutral templating route to mesoporous molecular sieves. *Science*, 267(5199), 865-867. <https://doi.org/10.1126/science.267.5199.865>
- Vance, K., Falzone G., Pignatelli I., Bauchy M., Balonis M., & Sant G. (2015). Direct carbonation of Ca(OH)₂ using liquid and supercritical CO₂: Implications for carbon-neutral cementation. *Industrial & Engineering Chemistry Research*, 54(36), 8908-8918. <https://doi.org/10.1021/acs.iecr.5b02356>
- Zarazua Aguilar Y., Paredes-Carrera, S.P., Sánchez-Ochoa, J. C., Avendaño-Gómez, J. R., Flores-Valle, S. O. (2017). Influence of microwave/ultrasound irradiation on the sol-gel synthesis of titanium dioxide nanoparticles for application in photocatalysis. *Revista Mexicana de Ingeniería Química*, 16(3), 899-909. <https://www.redalyc.org/pdf/620/62053304018.pdf>

- Zeyad, A. M., Tayeh, B. A., Adesina, A., de Azevedo, A. R., Amin, M., Hadzima-Nyarko, M., & Agwa, I. S. (2022). Review on effect of steam curing on behavior of concrete. *Cleaner Materials*, *3*, 100042. <https://doi.org/10.1016/j.clema.2022.100042>
- Zhao, D., Huo, Q., Feng, J., Chmelka, B. F., & Stucky, G. D. (1998). Nonionic triblock and star diblock copolymer and oligomeric surfactant syntheses of highly ordered, hydrothermally stable, mesoporous silica structures. *Journal of the American Chemical Society*, *120*(24), 6024-6036. <https://pubs.acs.org/doi/abs/10.1021/ja974025i>